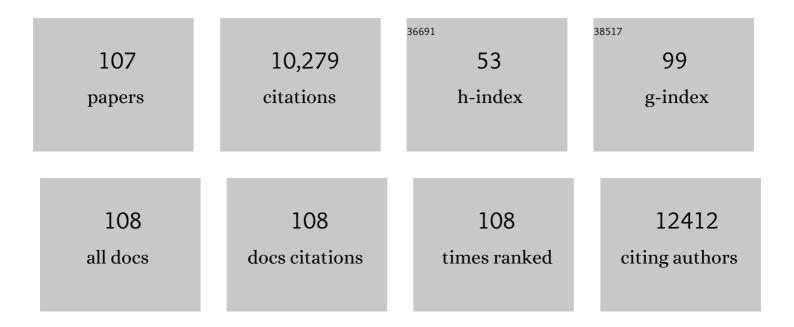
Guosheng Song

List of Publications by Year in descending order

Source: https://exaly.com/author-pdf/300666/publications.pdf Version: 2024-02-01



CHOSHENC SONC

#	Article	IF	CITATIONS
1	Recent development of magneto-optical nanoplatform for multimodality imaging of Pancreatic Ductal Adenocarcinoma. Nanoscale, 2022, , .	2.8	6
2	Chemical Design of Activatable Photoacoustic Probes for Precise Biomedical Applications. Chemical Reviews, 2022, 122, 6850-6918.	23.0	94
3	Dual key co-activated nanoplatform for switchable MRI monitoring accurate ferroptosis-based synergistic therapy. CheM, 2022, 8, 1956-1981.	5.8	67
4	Degradable Magnetic Nanoplatform with Hydroxide Ions Triggered Photoacoustic, MR Imaging, and Photothermal Conversion for Precise Cancer Theranostic. Nano Letters, 2022, 22, 3228-3235.	4.5	28
5	Ternary Alloy PtWMn as a Mn Nanoreservoir for Highâ€Field MRI Monitoring and Highly Selective Ferroptosis Therapy. Angewandte Chemie - International Edition, 2022, 61, .	7.2	53
6	Ratiometric afterglow luminescent nanoplatform enables reliable quantification and molecular imaging. Nature Communications, 2022, 13, 2216.	5.8	49
7	Ternary Alloy PtWMn as a Mn Nanoreservoir for Highâ€Field MRI Monitoring and Highly Selective Ferroptosis Therapy. Angewandte Chemie, 2022, 134, .	1.6	10
8	One-step reduction-encapsulated synthesis of Ag@polydopamine multicore-shell nanosystem for enhanced photoacoustic imaging and photothermal-chemodynamic cancer therapy. Nano Research, 2022, 15, 8291-8303.	5.8	8
9	Nanovoid-confinement and click-activated nanoreactor for synchronous delivery of prodrug pairs and precise photodynamic therapy. Nano Research, 2022, 15, 9264-9273.	5.8	10
10	Tongue cancer tailored photosensitizers for NIR-II fluorescence imaging guided precise treatment. Nano Today, 2022, 45, 101550.	6.2	31
11	Oxygen-embedded quinoidal acene based semiconducting chromophore nanoprobe for amplified photoacoustic imaging. Methods in Enzymology, 2021, 657, 385-413.	0.4	0
12	Engineering of magnetic nanoparticles as magnetic particle imaging tracers. Chemical Society Reviews, 2021, 50, 8102-8146.	18.7	64
13	<i>In Vivo</i> Imaging of Methionine Aminopeptidase II for Prostate Cancer Risk Stratification. Cancer Research, 2021, 81, 2510-2521.	0.4	8
14	An Acidityâ€Unlocked Magnetic Nanoplatform Enables Selfâ€Boosting ROS Generation through Upregulation of Lactate for Imagingâ€Guided Highly Specific Chemodynamic Therapy. Angewandte Chemie - International Edition, 2021, 60, 9562-9572.	7.2	140
15	An Acidityâ€Unlocked Magnetic Nanoplatform Enables Selfâ€Boosting ROS Generation through Upregulation of Lactate for Imagingâ€Guided Highly Specific Chemodynamic Therapy. Angewandte Chemie, 2021, 133, 9648-9658.	1.6	17
16	Manganese–Fluorouracil Metallodrug Nanotheranostic for MRI-Correlated Drug Release and Enhanced Chemoradiotherapy. CCS Chemistry, 2021, 3, 1116-1128.	4.6	13
17	Ratiometric Semiconducting Polymer Nanoparticle for Reliable Photoacoustic Imaging of Pneumonia-Induced Vulnerable Atherosclerotic Plaque in Vivo. Nano Letters, 2021, 21, 4484-4493.	4.5	51
18	Monitoring Immunotherapy With Optical Molecular Imaging. ChemMedChem, 2021, 16, 2547-2557.	1.6	6

#	Article	IF	CITATIONS
19	Tumorâ€&pecific Multipath Nucleic Acid Damages Strategy by Symbiosed Nanozyme@Enzyme with Synergistic Self yclic Catalysis. Small, 2021, 17, e2100766.	5.2	12
20	Cyclic Amplification of the Afterglow Luminescent Nanoreporter Enables the Prediction of Anti ancer Efficiency. Angewandte Chemie - International Edition, 2021, 60, 19779-19789.	7.2	42
21	Optical – Magnetic probe for evaluating cancer therapy. Coordination Chemistry Reviews, 2021, 441, 213978.	9.5	15
22	H ₂ S-Activated "One-Key Triple-Lock―Bis-Metal Coordination Network for Visualizing Precise Therapy of Colon Cancer. CCS Chemistry, 2021, 3, 2126-2142.	4.6	22
23	Cyclic Amplification of the Afterglow Luminescent Nanoreporter Enables the Prediction of Antiâ€cancer Efficiency. Angewandte Chemie, 2021, 133, 19932-19942.	1.6	6
24	Smart Nanozyme Platform with Activity orrelated Ratiometric Molecular Imaging for Predicting Therapeutic Effects. Angewandte Chemie - International Edition, 2021, 60, 26142-26150.	7.2	57
25	Two-dimensional intermetallic PtBi/Pt core/shell nanoplates overcome tumor hypoxia for enhanced cancer therapy. Nanoscale, 2021, 13, 14245-14253.	2.8	19
26	Generation of hydroxyl radical-activatable ratiometric near-infrared bimodal probes for early monitoring of tumor response to therapy. Nature Communications, 2021, 12, 6145.	5.8	66
27	<i>In vivo</i> therapeutic response monitoring by a self-reporting upconverting covalent organic framework nanoplatform. Chemical Science, 2020, 11, 1299-1306.	3.7	83
28	Specific Core–Satellite Nanocarriers for Enhanced Intracellular ROS Generation and Synergistic Photodynamic Therapy. ACS Applied Materials & Interfaces, 2020, 12, 5403-5412.	4.0	23
29	Reactive Oxygen Correlated Chemiluminescent Imaging of a Semiconducting Polymer Nanoplatform for Monitoring Chemodynamic Therapy. Nano Letters, 2020, 20, 176-183.	4.5	123
30	A two-photon fluorescence self-reporting black phosphorus nanoprobe for the <i>in situ</i> monitoring of therapy response. Chemical Communications, 2020, 56, 14007-14010.	2.2	10
31	Linkerâ€free Gold Nanoparticle Superstructure Coated with Poly(dopamine) by Siteâ€Specific Polymerization for Amplifying Photothermal Cancer Therapy. Chemistry - an Asian Journal, 2020, 15, 2742-2748.	1.7	9
32	Conjugated-Polymer-Based Nanomaterials for Photothermal Therapy. ACS Applied Polymer Materials, 2020, 2, 4258-4272.	2.0	65
33	Activatable Magnetic/Photoacoustic Nanoplatform for Redox-Unlocked Deep-Tissue Molecular Imaging <i>In Vivo</i> via Prussian Blue Nanoprobe. Analytical Chemistry, 2020, 92, 13452-13461.	3.2	28
34	Copper-thioguanine metallodrug with self-reinforcing circular catalysis for activatable MRI imaging and amplifying specificity of cancer therapy. Science China Chemistry, 2020, 63, 924-935.	4.2	29
35	Light-free Generation of Singlet Oxygen through Manganese-Thiophene Nanosystems for pH-Responsive Chemiluminescence Imaging and Tumor Therapy. CheM, 2020, 6, 2314-2334.	5.8	150
36	Oxygen-Embedded Pentacene Based Near-Infrared Chemiluminescent Nanoprobe for Highly Selective and Sensitive Visualization of Peroxynitrite In Vivo . Analytical Chemistry, 2020, 92, 4154-4163.	3.2	30

#	Article	IF	CITATIONS
37	Carbon-coated FeCo nanoparticles as sensitive magnetic-particle-imaging tracers with photothermal and magnetothermal properties. Nature Biomedical Engineering, 2020, 4, 325-334.	11.6	160
38	NIRâ€II Driven Plasmonâ€Enhanced Catalysis for a Timely Supply of Oxygen to Overcome Hypoxiaâ€Induced Radiotherapy Tolerance. Angewandte Chemie - International Edition, 2019, 58, 15069-15075.	7.2	142
39	Nitric Oxide-Activated "Dual-Key–One-Lock―Nanoprobe for in Vivo Molecular Imaging and High-Specificity Cancer Therapy. Journal of the American Chemical Society, 2019, 141, 13572-13581.	6.6	126
40	Oxygen-Embedded Quinoidal Acene Based Semiconducting Chromophore Nanoprobe for Amplified Photoacoustic Imaging and Photothermal Therapy. Analytical Chemistry, 2019, 91, 15275-15283.	3.2	28
41	NIRâ€II Driven Plasmonâ€Enhanced Catalysis for a Timely Supply of Oxygen to Overcome Hypoxiaâ€Induced Radiotherapy Tolerance. Angewandte Chemie, 2019, 131, 15213-15219.	1.6	19
42	Nanoscale Metal–Organic Framework Based Two-Photon Sensing Platform for Bioimaging in Live Tissue. Analytical Chemistry, 2019, 91, 2727-2733.	3.2	63
43	A Review of Magnetic Particle Imaging and Perspectives on Neuroimaging. American Journal of Neuroradiology, 2019, 40, 206-212.	1.2	133
44	A Magneto-Optical Nanoplatform for Multimodality Imaging of Tumors in Mice. ACS Nano, 2019, 13, 7750-7758.	7.3	78
45	Persistent Regulation of Tumor Microenvironment via Circulating Catalysis of MnFe ₂ O ₄ @Metal–Organic Frameworks for Enhanced Photodynamic Therapy. Advanced Functional Materials, 2019, 29, 1901417.	7.8	217
46	Bright sub-20-nm cathodoluminescent nanoprobes for electron microscopy. Nature Nanotechnology, 2019, 14, 420-425.	15.6	36
47	Magnetic Particle Imaging in Neurosurgery. World Neurosurgery, 2019, 125, 261-270.	0.7	31
48	Two-Photon Supramolecular Nanoplatform for Ratiometric Bioimaging. Analytical Chemistry, 2019, 91, 6371-6377.	3.2	24
49	A dual factor activated metal–organic framework hybrid nanoplatform for photoacoustic imaging and synergetic photo-chemotherapy. Nanoscale, 2019, 11, 20630-20637.	2.8	39
50	Degradable rhenium trioxide nanocubes with high localized surface plasmon resonance absorbance like gold for photothermal theranostics. Biomaterials, 2018, 159, 68-81.	5.7	52
51	Smart Nanoreactors for pH-Responsive Tumor Homing, Mitochondria-Targeting, and Enhanced Photodynamic-Immunotherapy of Cancer. Nano Letters, 2018, 18, 2475-2484.	4.5	348
52	Janus Iron Oxides @ Semiconducting Polymer Nanoparticle Tracer for Cell Tracking by Magnetic Particle Imaging. Nano Letters, 2018, 18, 182-189.	4.5	168
53	Catalase-loaded cisplatin-prodrug-constructed liposomes to overcome tumor hypoxia for enhanced chemo-radiotherapy of cancer. Biomaterials, 2017, 138, 13-21.	5.7	214
54	Bottomâ€Up Preparation of Uniform Ultrathin Rhenium Disulfide Nanosheets for Imageâ€Guided Photothermal Radiotherapy. Advanced Functional Materials, 2017, 27, 1700250.	7.8	100

#	Article	IF	CITATIONS
55	Emerging Nanotechnology and Advanced Materials for Cancer Radiation Therapy. Advanced Materials, 2017, 29, 1700996.	11.1	528
56	Drugâ€Loaded Mesoporous Tantalum Oxide Nanoparticles for Enhanced Synergetic Chemoradiotherapy with Reduced Systemic Toxicity. Small, 2017, 13, 1602869.	5.2	62
57	Design and Functionalization of the NIR-Responsive Photothermal Semiconductor Nanomaterials for Cancer Theranostics. Accounts of Chemical Research, 2017, 50, 2529-2538.	7.6	312
58	Chelator-Free Labeling of Metal Oxide Nanostructures with Zirconium-89 for Positron Emission Tomography Imaging. ACS Nano, 2017, 11, 12193-12201.	7.3	34
59	Liposomes co-loaded with metformin and chlorin e6 modulate tumor hypoxia during enhanced photodynamic therapy. Nano Research, 2017, 10, 1200-1212.	5.8	128
60	TaOx decorated perfluorocarbon nanodroplets as oxygen reservoirs to overcome tumor hypoxia and enhance cancer radiotherapy. Biomaterials, 2017, 112, 257-263.	5.7	199
61	Combined bortezomib-based chemotherapy and p53 gene therapy using hollow mesoporous silica nanospheres for p53 mutant non-small cell lung cancer treatment. Biomaterials Science, 2017, 5, 77-88.	2.6	59
62	Drug-induced co-assembly of albumin/catalase as smart nano-theranostics for deep intra-tumoral penetration, hypoxia relieve, and synergistic combination therapy. Journal of Controlled Release, 2017, 263, 79-89.	4.8	165
63	In Vivo Longâ€Term Biodistribution, Excretion, and Toxicology of PEGylated Transitionâ€Metal Dichalcogenides MS ₂ (M = Mo, W, Ti) Nanosheets. Advanced Science, 2017, 4, 1600160.	5.6	191
64	Catalaseâ€Loaded TaOx Nanoshells as Bioâ€Nanoreactors Combining Highâ€Z Element and Enzyme Delivery for Enhancing Radiotherapy. Advanced Materials, 2016, 28, 7143-7148.	11.1	346
65	Hyaluronidase To Enhance Nanoparticle-Based Photodynamic Tumor Therapy. Nano Letters, 2016, 16, 2512-2521.	4.5	279
66	Au@MnS@ZnS Core/Shell/Shell Nanoparticles for Magnetic Resonance Imaging and Enhanced Cancer Radiation Therapy. ACS Applied Materials & Interfaces, 2016, 8, 9557-9564.	4.0	70
67	Hierarchical Heterostructures of NiCo2O4@XMoO4 (X = Ni, Co) as an Electrode Material for High-Performance Supercapacitors. Nanoscale Research Letters, 2016, 11, 257.	3.1	28
68	Allâ€inâ€One Theranostic Nanoplatform Based on Hollow TaOx for Chelatorâ€Free Labeling Imaging, Drug Delivery, and Synergistically Enhanced Radiotherapy. Advanced Functional Materials, 2016, 26, 8243-8254.	7.8	78
69	Core–shell Au@MnO2 nanoparticles for enhanced radiotherapy via improving the tumor oxygenation. Nano Research, 2016, 9, 3267-3278.	5.8	155
70	Ultra-small MoS2 nanodots with rapid body clearance for photothermal cancer therapy. Nano Research, 2016, 9, 3003-3017.	5.8	134
71	Ultrafine MnO2 Nanowire Arrays Grown on Carbon Fibers for High-Performance Supercapacitors. Nanoscale Research Letters, 2016, 11, 469.	3.1	24
72	FeSe ₂ â€Decorated Bi ₂ Se ₃ Nanosheets Fabricated via Cation Exchange for Chelatorâ€Free ⁶⁴ Cuâ€Labeling and Multimodal Imageâ€Guided Photothermalâ€Radiation Therapy. Advanced Functional Materials, 2016, 26, 2185-2197.	7.8	225

#	Article	IF	CITATIONS
73	Perfluorocarbonâ€Loaded Hollow Bi ₂ Se ₃ Nanoparticles for Timely Supply of Oxygen under Nearâ€Infrared Light to Enhance the Radiotherapy of Cancer. Advanced Materials, 2016, 28, 2716-2723.	11.1	518
74	Cancer Therapy: Perfluorocarbon-Loaded Hollow Bi2 Se3 Nanoparticles for Timely Supply of Oxygen under Near-Infrared Light to Enhance the Radiotherapy of Cancer (Adv. Mater. 14/2016). Advanced Materials, 2016, 28, 2654-2654.	11.1	10
75	Degradable Molybdenum Oxide Nanosheets with Rapid Clearance and Efficient Tumor Homing Capabilities as a Therapeutic Nanoplatform. Angewandte Chemie - International Edition, 2016, 55, 2122-2126.	7.2	254
76	Emerging nanomedicine approaches fighting tumor metastasis: animal models, metastasis-targeted drug delivery, phototherapy, and immunotherapy. Chemical Society Reviews, 2016, 45, 6250-6269.	18.7	365
77	Degradable Molybdenum Oxide Nanosheets with Rapid Clearance and Efficient Tumor Homing Capabilities as a Therapeutic Nanoplatform. Angewandte Chemie, 2016, 128, 2162-2166.	1.6	12
78	NaYF ₄ :Yb/Er@PPy core–shell nanoplates: an imaging-guided multimodal platform for photothermal therapy of cancers. Nanoscale, 2016, 8, 1040-1048.	2.8	42
79	Core–Shell MnSe@Bi ₂ Se ₃ Fabricated via a Cation Exchange Method as Novel Nanotheranostics for Multimodal Imaging and Synergistic Thermoradiotherapy. Advanced Materials, 2015, 27, 6110-6117.	11.1	330
80	Magnetic Fieldâ€Enhanced Photothermal Ablation of Tumor Sentinel Lymph Nodes to Inhibit Cancer Metastasis. Small, 2015, 11, 4856-4863.	5.2	36
81	Imagingâ€Guided Combined Photothermal and Radiotherapy to Treat Subcutaneous and Metastatic Tumors Using Iodineâ€131â€Doped Copper Sulfide Nanoparticles. Advanced Functional Materials, 2015, 25, 4689-4699.	7.8	207
82	Adsorption of Billl on Pt nanoparticles leading to the enhanced electrocatalysis of glucose oxidation. Colloid Journal, 2015, 77, 382-389.	0.5	10
83	MoS ₂ -Based Nanoprobes for Detection of Silver Ions in Aqueous Solutions and Bacteria. ACS Applied Materials & Interfaces, 2015, 7, 7526-7533.	4.0	85
84	Synthesis of Uniform Platinum Nanoparticles Using Glucose as Dispersant. Nanoscience and Nanotechnology Letters, 2014, 6, 592-595.	0.4	4
85	A newly prepared Ni(OH)2@Cr(OH)3 nanohybrid for its bioelectrocatalysis. Sensors and Actuators B: Chemical, 2014, 198, 350-359.	4.0	11
86	The use of hollow mesoporous silica nanospheres to encapsulate bortezomib and improve efficacy for non-small cell lung cancer therapy. Biomaterials, 2014, 35, 316-326.	5.7	96
87	Cu _{2â^'x} Se@mSiO ₂ –PEG core–shell nanoparticles: a low-toxic and efficient difunctional nanoplatform for chemo-photothermal therapy under near infrared light radiation with a safe power density. Nanoscale, 2014, 6, 4361-4370.	2.8	77
88	A Novel Photothermal Nanocrystals of Cu7S4 Hollow Structure for Efficient Ablation of Cancer Cells. Nano-Micro Letters, 2014, 6, 169-177.	14.4	33
89	Hydrophilic Molybdenum Oxide Nanomaterials with Controlled Morphology and Strong Plasmonic Absorption for Photothermal Ablation of Cancer Cells. ACS Applied Materials & Interfaces, 2014, 6, 3915-3922.	4.0	166
90	Facile synthesis of porous MnCo ₂ O _{4.5} hierarchical architectures for high-rate supercapacitors. CrystEngComm, 2014, 16, 2335-2339.	1.3	131

#	Article	IF	CITATIONS
91	One-pot morphology-controlled synthesis of various shaped mesoporous silica nanoparticles. Journal of Materials Science, 2013, 48, 5718-5726.	1.7	49
92	In situ synthesis of P3HT-capped CdSe superstructures and their application in solar cells. Nanoscale Research Letters, 2013, 8, 106.	3.1	25
93	Surface decoration of Bi2WO6 superstructures with Bi2O3 nanoparticles: an efficient method to improve visible-light-driven photocatalytic activity. CrystEngComm, 2013, 15, 9011.	1.3	75
94	Ultrathin PEGylated W ₁₈ O ₄₉ Nanowires as a New 980 nm‣aserâ€Driven Photothermal Agent for Efficient Ablation of Cancer Cells In Vivo. Advanced Materials, 2013, 25, 2095-2100.	11.1	370
95	Phase-controlled synthesis and photocatalytic properties of SnS, SnS2 and SnS/SnS2 heterostructure nanocrystals. Materials Research Bulletin, 2013, 48, 2325-2332.	2.7	87
96	Self-assembling hybrid NiO/Co3O4 ultrathin and mesoporous nanosheets into flower-like architectures for pseudocapacitance. Journal of Materials Chemistry A, 2013, 1, 9107.	5.2	101
97	Nanocomposites: A Low-Toxic Multifunctional Nanoplatform Based on Cu9S5@mSiO2Core-Shell Nanocomposites: Combining Photothermal- and Chemotherapies with Infrared Thermal Imaging for Cancer Treatment (Adv. Funct. Mater. 35/2013). Advanced Functional Materials, 2013, 23, 4280-4280.	7.8	8
98	A Lowâ€Toxic Multifunctional Nanoplatform Based on Cu ₉ S ₅ @mSiO ₂ Coreâ€Shell Nanocomposites: Combining Photothermal―and Chemotherapies with Infrared Thermal Imaging for Cancer Treatment. Advanced Functional Materials, 2013, 23, 4281-4292.	7.8	207
99	MnO2 ultralong nanowires with better electrical conductivity and enhanced supercapacitor performances. Journal of Materials Chemistry, 2012, 22, 14864.	6.7	101
100	Phase-controlled synthesis and gas-sensing properties of zinc stannate (ZnSnO3 and Zn2SnO4) faceted solid and hollow microcrystals. CrystEngComm, 2012, 14, 2172.	1.3	89
101	A simple transformation from silica core–shell–shell to yolk–shell nanostructures: a useful platform for effective cell imaging and drug delivery. Journal of Materials Chemistry, 2012, 22, 17011.	6.7	37
102	One-step aqueous solution synthesis of Ge nanocrystals from GeO2 powders. CrystEngComm, 2011, 13, 3674.	1.3	37
103	Highly aligned SnO2 nanorods on graphene sheets for gas sensors. Journal of Materials Chemistry, 2011, 21, 17360.	6.7	199
104	A Zn2GeO4–ethylenediamine hybrid nanoribbon membrane as a recyclable adsorbent for the highly efficient removal of heavy metals from contaminated water. Chemical Communications, 2011, 47, 10719.	2.2	51
105	A Mobile Sn Nanowire Inside a <i>βâ€</i> Ga ₂ O ₃ Tube: A Practical Nanoscale Electrically/Thermally Driven Switch. Small, 2011, 7, 3377-3384.	5.2	10
106	Smart Nanozyme Platform with Activityâ€Correlated Ratiometric Molecular Imaging for Predicating Therapeutic Effect. Angewandte Chemie, 0, , .	1.6	6
107	Magnetic-Optical Imaging for Monitoring Chemodynamic Therapy. Chemical Research in Chinese Universities, 0, , 1.	1.3	1